We are IntechOpen, the world's leading publisher of Open Access books
Built by scientists, for scientists

6,900
Open access books available

185,000
International authors and editors

200M
Downloads

154
Countries delivered to

Our authors are among the

TOP 1%
most cited scientists

12.2%
Contributors from top 500 universities

CLARIVATE ANALYTICS
BOOK CITATION INDEX
INDEXED

WEB OF SCIENCE™

Selection of our books indexed in the Book Citation Index
in Web of Science™ Core Collection (BKCI)

Interested in publishing with us?
Contact book.department@intechopen.com

Magnetically Coupled Resonance Wireless Power Transfer (MR-WPT) with Multiple Self-Resonators

Youngjin Park, Jinwook Kim and Kwan-Ho Kim
Korea Electrotechnology Research Institute (KERI) and
University of Science & Technology (UST)
Republic of Korea

1. Introduction

Wireless power transfer (WPT) has been studied for more than one hundred years since Nikola Tesla proposed his WPT concept. As more and more portable electronic devices and consumer electronics are developed and used, the need for WPT technology will continue to grow.
Recently, WPT via strongly coupled magnetic resonances in the near field has been reported by Kurs et al. (2007). The basic principle of WPT based on magnetically coupled resonance (MR-WPT) is that two self-resonators that have the same resonant frequency can transfer energy efficiently over midrange distances. It was also reported that MR-WPT has several valuable advantages, such as efficient midrange power transfer, non-radiative, and nearly omnidirectional. It is certain that these properties will help to improve the performance of current wireless power transfer systems and be utilized well for various wireless power transfer applications such as electric vehicles, consumer electronics, smart mobile devices, biomedical implants, robots, and so on.
Up to now, several important articles have been published. Karalis et al. (2008) reported detailed physical phenomena of efficient wireless non-radiative mid-range energy transfer. Sample et al. (2010) reported an equivalent model and analysis of an MR-WPT system using circuit theory, and Hamam et al. (2009) introduced an MR-WPT system that used an intermediate self-resonator coil to extend the coverage of wireless power transfer that is coaxially arranged with both Tx and Rx self-resonant coils.
In Figure 1, a practical application model of wireless power charging of multiple portable electronic devices using MR-WPT technology is illustrated. Multiple devices are placed on the Rx self-resonator, which is built into the desk, and the Tx self-resonator is built into the power plate wall. The Tx self-resonator is strongly coupled with the Rx one and then both Tx and Rx self-resonators transfer energy efficiently even though the Tx self-resonator is geometrically perpendicular to the Rx self-resonator. In order to create this system, it is necessary to characterize power transfer efficiency and especially mutual inductance of the MR-WPT system with two self-resonators arranged perpendicularly. However, there have been few research reports published that analyze the characteristics of MR-WPT regarding a geometrical arrangement between Tx and Rx self-resonators and between Tx or Rx and intermediate self-resonators.
In this article, the characteristics of wireless power transfer between two self-resonators arranged in off-axis positions are reported and the power transfer efficiency of an MR-WPT

system with an intermediate self-resonator is analyzed. The intermediate self-resonator is geometrically perpendicular or coaxial to the Tx and Rx self-resonators. To calculate the power transfer efficiency, a modified coupled mode theory (CMT) is applied. In particular, a calculation method and analysis results of mutual inductance between two self-resonators arranged in off-axis positions are presented.
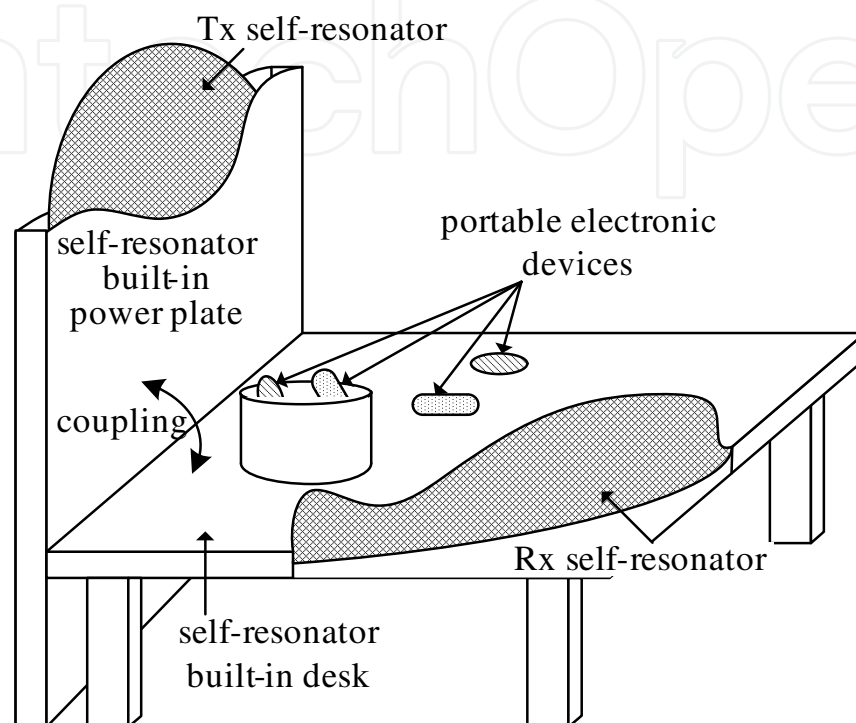

Fig. 1. A practical application of a wireless power transfer system using MR-WPT.

The article is organized as follows. In Section 2, the configuration and modeling of an MR-WPT system with an intermediate self-resonator is illustrated and the power transfer efficiency of the system is derived. In Section 3, mutual inductance between two self-resonators is derived for rectangular and circular coils. In Section 4, two MR-WPT systems with intermediate self-resonators are fabricated and formula derivation, analysis results, and design procedures are verified by experimental measurement.

2. Illustration and modeling of an MR-WPT system with an intermediate self-resonator

Figure 2 shows the configuration of an MR-WPT system with multiple self-resonators. It consists of three self-resonators (Tx, Rx, and intermediate), a source coil, and a load coil. The centers of the Tx, Rx, and intermediate self-resonators are $(0, 0, -D_{1m})$, $(0, 0, D_{2m})$, and $(-D_h, 0, 0)$, respectively. Each coil is loaded with a series of high Q capacitors in order to adjust the target resonant frequency and prevent change of the resonant frequency due to unknown objects. It should be noted that the intermediate resonant coil is arranged perpendicularly with both Tx and Rx self-resonators. By referring to Haus (1984) and Hamam et al. (2009), a
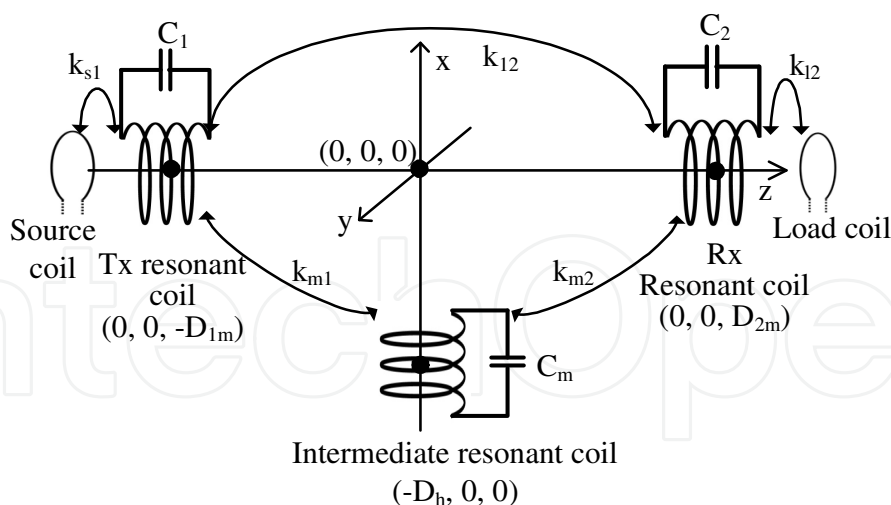
Fig. 2. Configuration of an MR-WPT system with an intermediate self-resonator.

modified CMT equation in matrix form can be written as:

$$
\begin{pmatrix}
\frac{d}{dt}a_1(t) \\
\frac{d}{dt}a_m(t) \\
\frac{d}{dt}a_2(t) \\
S_{-1} \\
S_{-2}
\end{pmatrix}
=
\begin{pmatrix}
-(i\omega_1 + \Gamma_1) - k_{s1} & ik_{1m} & ik_{12} & \sqrt{2k_{s1}} & 0 \\
iM_{m1} & -(i\omega_m + \Gamma_m) & ik_{m2} & 0 & 0 \\
ik_{12} & ik_{2m} & -(i\omega_2 + \Gamma_2) - k_{l2} & 0 & 0 \\
\sqrt{2k_{s1}} & 0 & 0 & -1 & 0 \\
0 & 0 & \sqrt{2k_{l2}} & 0 & 0
\end{pmatrix}
\begin{pmatrix}
a_1(t) \\
a_m(t) \\
a_2(t) \\
S_{+1} \\
S_{+2}
\end{pmatrix}.
$$

(1)

k_{s1}, k_{l2}, k_{m1}, k_{m2}, and k_{12} are coupling coefficients between coils. The parameters are defined as follows:

- $a_i(t)$: mode amplitude of each self-resonator,

- ω_i : angular resonant frequency of each self-resonator, $1/\sqrt{L_i C_i}$,

- Γ_i : intrinsic decay rate of each self-resonator, $R_i/2L_i$,

- L_i and R_i : self-inductance and resistance of each self-resonator,

- C_i: capacitance of each self-resonator (self-capacitance + high-Q capacitor),

- k_{ij} : coupling coefficient between i and j self-resonators, $\omega M_{ij}/2\sqrt{L_i L_j}$,

- M_{ij} : mutual inductance between i and j self-resonators,

- $S_{\pm 1}$: field amplitude of an incident field $(+)$ and a reflected field $(-)$ at the source,

- $S_{\pm 2}$: field amplitude of an incident field $(+)$ and a reflected field $(-)$ at the load,

- i and $j(= 1, 2, m, s, l)$: 1 (Tx self-resonator), 2 (Rx self-resonator), m (intermediate self-resonator), s (source coil), l (load coil).

To simplify Equation 1, it is assumed that $k_{12} \approx 0, \Gamma_1 = \Gamma_2 = \Gamma \neq \Gamma_m$, and $k_{m1} = k_{m2} = k_m$. That is, Tx and Rx self-resonators are identical and the intermediate self-resonator is placed at the center of the Tx and Rx self-resonators ($D_{1m} = D_{2m}$). Also, the coupling coefficient k_m is

much higher than k_{12}. Then, the transmission coefficient (S_{21}) from source to load is obtained as:

$$S_{21} = \frac{-2U_m^2 U_0}{[1 + U_0 - iX_1][1 + U_0 - iX_2][1 - iX_m] + U_m^2[2(1 + U_0) - i(X_1 + X_2)]}, \tag{2}$$

where $X_1 = X_2 = (\omega_{1,2} - \omega_0)/\Gamma$, $X_m = (\omega_m - \omega_0)/\Gamma_m$, $U_0 = k_{s1}/\Gamma = k_{l2}/\Gamma$, $U_m = \sqrt{k_m^2/\Gamma\Gamma_m}$, and ω_0 is a target angular resonant frequency. Then, the power transfer efficiency η is obtained as:

$$\eta = |S_{21}|^2. \tag{3}$$

By assuming that the resonant frequency of each self-resonator is the same as the target resonant frequency, that is, $X_1 = X_2 = X_m = 0$, the matching condition for maximum power transfer efficiency in Equation 1 is obtained as:

$$U_0^{opt} = \sqrt{1 + 2U_m^2}.$$

The maximum power transfer efficiency using the condition is rewritten as follows:

$$\eta = \frac{(k_m^2/\Gamma\Gamma_m)^2}{(\sqrt{1 + 2k_m^2/\Gamma\Gamma_m} + 1 + k_m^2/\Gamma\Gamma_m)^2} = \frac{U_m^4}{(\sqrt{1 + 2U_m^2} + 1 + U_m^2)^2}. \tag{4}$$

To calculate Equation 4, three unknown parameters of k_m, Γ, and Γ_m should be determined. The intrinsic decay rates of Γ and Γ_m are determined by the resistance and inductance of each self-resonator. k_m is calculated by mutual inductance between two self-resonators and the self-inductance of each self-resonator. It can also be noted that proper matching in an MR-WPT system with k_m fixed can be accomplished by varying k_{l2} for maximum power transfer.

In the next section, the calculation method of mutual inductance is presented for the case of circular and rectangular types of self-resonators.

3. Derivation of mutual inductance

3.1 Mutual inductance between two circular self-resonators
3.1.1 Configuration and derivation

In Figure 3, two circular self-resonators are arranged coaxially and perpendicularly. D is the distance between two coils. For the calculation of mutual inductance, it is assumed that the coils are filamentary and current is uniformly distributed on the coils. Mutual inductance M_{12} between two coils is written as:

$$M_{12} = \frac{N_1 N_2}{I} \int_{S_2} \vec{B} \cdot d\vec{s_2}. \tag{5}$$

By referring to Good (2001), the magnetic flux density, $\vec{B}$ at arbitrary spatial points is written as follows:

$$\vec{B} = \hat{\rho} B_\rho + \hat{z} B_z, \tag{6a}$$

where

$$B_z|_{\rho=0} = \frac{\mu_0 I r_1^2}{2(D^2 + r_1^2)^{3/2}},$$

$$B_z|_{\rho\neq0} = \frac{\mu_0 I}{2\pi\rho}\left(\frac{m}{4r_1\rho}\right)^{1/2}\left(\rho K(m) - \frac{r_1 m - (2-m)\rho}{2(1-m)}E(m)\right), \qquad (6b)$$

$$B_\rho|_{\rho\neq0} = \frac{\mu_0 I D}{2\pi\rho}\left(\frac{m}{4r_1\rho}\right)^{1/2}\left(-K(m) + \frac{2-m}{2(1-m)}E(m)\right),$$

with

$$K(m) = \int_0^{\pi/2}(1 - m\cdot\sin^2\theta)^{-1/2}d\theta,$$

$$E(m) = \int_0^{\pi/2}(1 - m\cdot\sin^2\theta)^{1/2}d\theta, \qquad (6c)$$

$$m = \frac{4r_1\rho}{(r_1 + \rho)^2 + D^2}.$$

Here, K and E are the complete elliptic integrals of the first and second kinds, respectively. m is the variable of elliptic integrals. N_1 and N_2 are the number of turns of the first and second coils, respectively. In the coaxially arranged system (see Figure 3a), mutual inductance is determined by only z-directed fields (B_z). The magnetic flux density of a circular coil at the points of the same ρ is identical and then the total magnetic flux linkage is obtained by summing the flux of a central circular area and each circular subdivision as well. Therefore, by assuming that N_d is sufficiently large, mutual inductance between two coaxially arranged coils is written as follows:

$$M_{cc} = \frac{2\pi d^2 N_1 N_2}{I}\left\{\frac{B_z|_{n=0}}{4} + \sum_{n=1}^{N_d=r_2/d} nB_z|_n\right\} \approx \frac{2\pi d^2 N_1 N_2}{I}\sum_{n=1}^{N_d=r_2/d} nB_z|_n. \qquad (7)$$

Here, N_d is the total number of subdivisions of the Rx self-resonator.
For the case of two perpendicularly arranged circular coils (see Figure 3b), mutual inductance is determined by only ρ-directed fields. Therefore, the mutual inductance is obtained as follows:

$$M_{pc} = \frac{N_1 N_2}{I}\sum_{n=1}^{N_d=2r_2/d} B_\rho|_n \cdot S_n, \qquad (8)$$

where $S_n = 2nd^2\sqrt{2r_2/nd - 1}$ and is the n-th rectangular area subdivided. For more general cases, see Babic et al. (2010).

3.1.2 Calculation and measurement

For verification of the calculation method, two self-resonators were made as shown in Figures 4 and 10. A target resonant frequency, f_0 was 1.25 MHz. The Tx self-resonator was a helical type ($r = 252$ mm, $H = 90$ mm, $N_1 = 9$ turns, $a = 2.2$ mm). The Rx coil was a spiral type ($r_{in} = 230$ mm, $r_{out} = 300$ mm, $N_2 = 10$ turns, $a = 3.2$ mm). Both of the coils were made of copper pipe ($\sigma = 5.8 \times 10^7$). Using high-Q capacitors, the target resonant frequency of each self-resonator was adjusted. The intrinsic decay rate using measured resistance and inductance, capacitance of high-Q capacitors for each self-resonator, self-inductances, and resonant frequencies of the self-resonators are shown in Table 1. To measure resonant
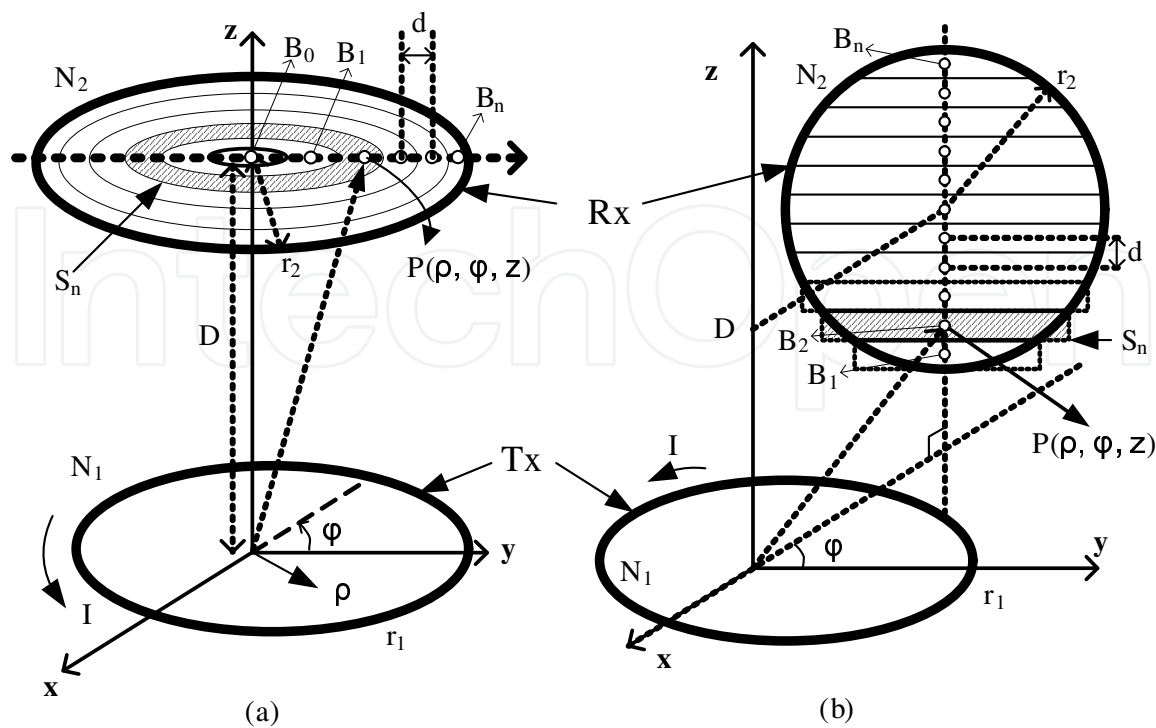
Fig. 3. Configuration of two circular self-resonators for calculation of mutual inductance.

frequency, a vector network analyzer (Agilent 4395A) was used. To measure self-inductance (L) and resistance (R) of each self-resonator, an LCR meter (GWInstek 8110G) was used.
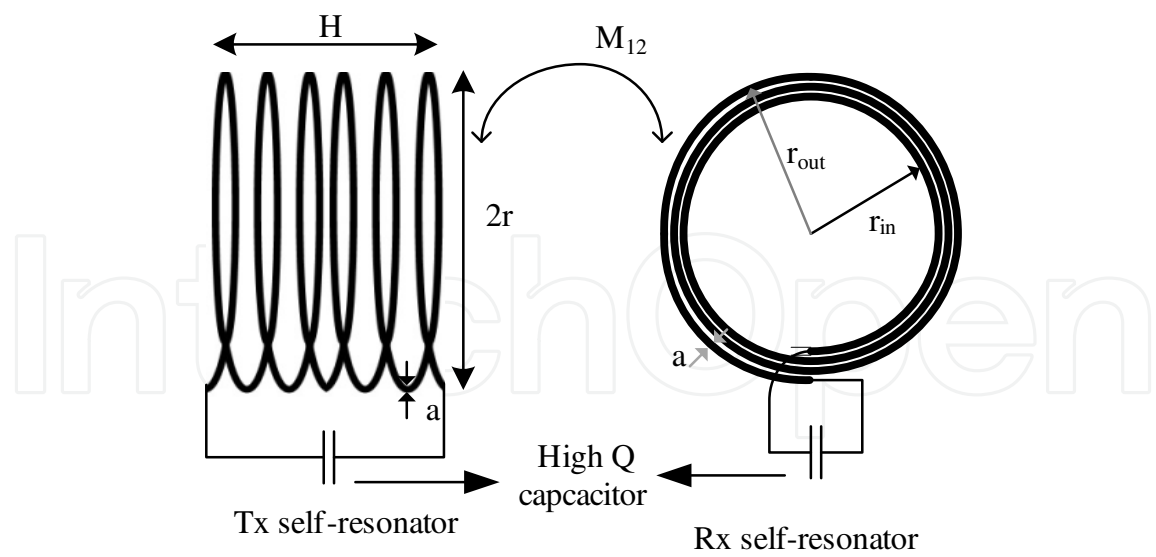

Fig. 4. Schematic drawing of Tx and Rx self-resonators.

To measure mutual inductance, both differential coupling inductance ($L_{m1} = L_1 + L_2 - 2M_{12}$) and cumulative coupling inductance ($L_{m2} = L_1 + L_2 + 2M_{12}$) were measured and then the

	Γ	High-Q capacitor	self-inductance	f_0
Tx (helix)	8168.14	224.40 pF	67.00 uH	1.2525 MHz
Rx (spiral)	8325.22	221.00 pF	98.82 uH	1.2494 MHz

Table 1. Summary of measured parameters of each self-resonator.

mutual inductance was obtained as follows Hayes et al. (2003):

$$M_{12} = \frac{|L_{m1} - L_{m2}|}{4}. \tag{9}$$

Figure 5 shows the theoretical and experimental mutual inductance according to the distance (D) between two self-resonators. In a perpendicular arrangement, the $\rho-$directed position is fixed at $\rho = 230$ mm. For both coaxial and perpendicular arrangements, the calculated results have good agreement with the measured ones. For the perpendicular case, there is a slight difference between calculation and measurement, especially as the two coils become closer, because the magnetic flux density at each subdivision is not uniform. It can be observed that the mutual inductance for the coaxial case is higher than that for the perpendicular case.
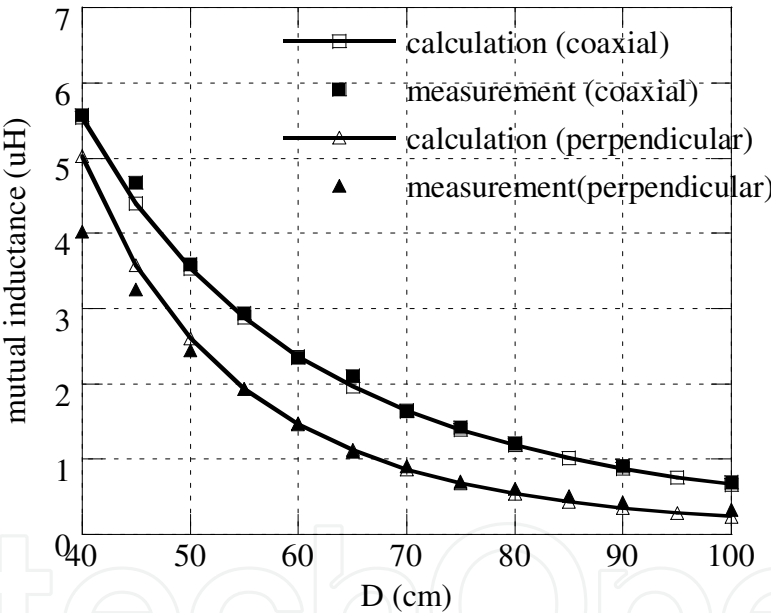

Fig. 5. Calculation and measurement of mutual inductance for both coaxial and perpendicular arrangements.

3.2 Mutual inductance between two rectangular self-resonators
3.2.1 Configuration and derivation
Figure 6 shows a geometrical configuration used to calculate mutual inductance between two rectangular self-resonators arranged in an off-axis position. The Tx coil is placed on the xy plane and its center is $(0,0,0)$. It has N_1 turns. It is L_1 in width and h_1 in height, respectively. The center of the Rx coil is $P_0(x_0, y_0, z_0)$ and the coil is parallel to the $y-$axis. The Rx coil has N_2 turns. It is L_2 in width and h_2 in height, respectively. Tx and Rx coils are tilted θ degrees. It is assumed that each coil is filamentary. To calculate mutual inductance between Tx and
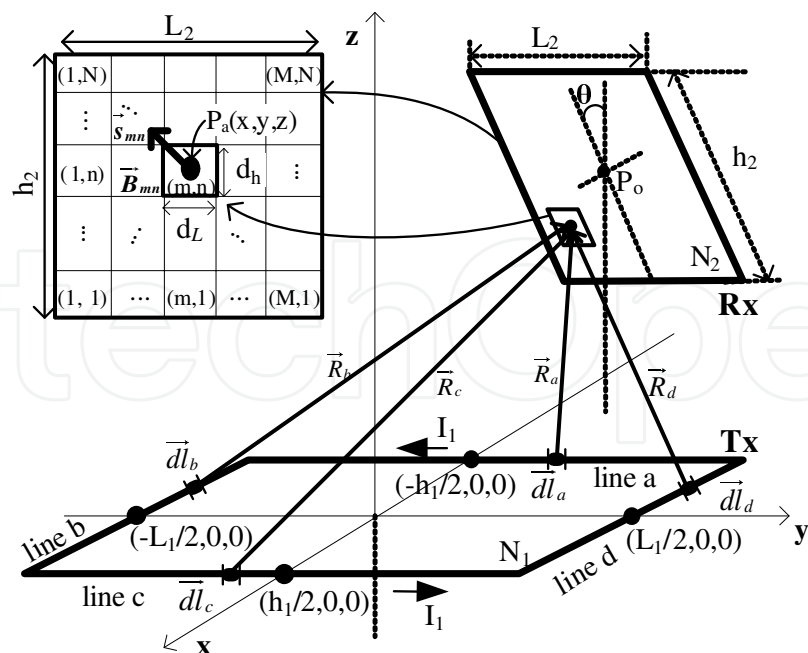
Fig. 6. Configuration of two rectangular self-resonators for calculation of mutual inductance.

Rx self-resonators, the rectangular Tx self-resonator is divided into four lines (line a, line b, line c, line d) and the Rx self-resonator is subdivided (see Figure 6). A subdivision (m, n) is rectangular and its midpoint is $P_a(x, y, z)$. The magnetic flux density at each point $P_a(x, y, z)$ of the subdivision in the Rx self-resonator can be obtained by combining the magnetic flux densities made by the four lines of the Tx self-resonator. It is assumed that $\vec{B}_{mn}$ is uniform in each subdivision. Therefore, by referring to the case of the circular self-resonator in the previous section, the mutual inductance M_{rc} is calculated as follows:

$$M_{12} = M_{rc} = \frac{N_1 N_2}{I_1} \int_{S_2} \vec{B} \cdot d\vec{s}_2 \approx \frac{N_1 N_2}{I_1} \sum_{m=1}^{M} \sum_{n=1}^{N} \vec{B}_{mn} \cdot \vec{s}_{mn}. \tag{10}$$

$\vec{s}_{mn}$ is the surface of the subdivision (m, n). The magnetic flux density at each subdivision $\vec{B}_{mn}$ is obtained using Bio-Savart's law. The $y-$directed magnetic fields $\hat{y}B_{y_{mn}}$ will not be affected by the mutual inductance due to $\hat{y}B_{y_{mn}} \cdot \vec{s}_{mn} = 0$. Therefore, $\vec{B}_{mn}$ is obtained as follows:

$$\begin{aligned}
\vec{B}_{mn} &= \frac{\mu_0 I_1}{4\pi} \oint_{C_{Tx}} \left(\frac{d\vec{l'} \times \vec{R}}{R^3} \right) \\
&= \frac{\mu_0 I_1}{4\pi} \left\{ \int_{line\,a} \frac{d\vec{l}_a \times \vec{R}_a}{R_a^3} + \int_{line\,b} \frac{d\vec{l}_b \times \vec{R}_b}{R_b^3} + \int_{line\,c} \frac{d\vec{l}_c \times \vec{R}_c}{R_c^3} + \int_{line\,d} \frac{d\vec{l}_d \times \vec{R}_d}{R_d^3} \right\} \\
&= \hat{x}B_{x_{mn}} + \hat{z}B_{z_{mn}},
\end{aligned} \tag{11a}$$

where

$$\begin{aligned}
B_{x_{mn}} &= B_x|_{line\,a} + B_x|_{line\,c}, \\
B_{z_{mn}} &= B_z|_{line\,a} + B_z|_{line\,b} + B_z|_{line\,c} + B_z|_{line\,d},
\end{aligned} \tag{11b}$$

with

$$B_x|_{line\,a} = \frac{\mu_0}{4\pi}\left(\frac{-zI_1}{(x+h_1/2)^2+z^2}\right)\left[\left(\frac{y+L_1/2}{R_{a+}}\right)-\left(\frac{y-L_1/2}{R_{a-}}\right)\right],$$

$$B_x|_{line\,c} = \frac{\mu_0}{4\pi}\left(\frac{zI_1}{(x-h_1/2)^2+z^2}\right)\left[\left(\frac{y+L_1/2}{R_{c+}}\right)-\left(\frac{y-L_1/2}{R_{c-}}\right)\right],$$

$$B_z|_{line\,a} = \frac{\mu_0}{4\pi}\left(\frac{I_1(x+h_1/2)}{(x+h_1/2)^2+z^2}\right)\left[\left(\frac{y+L_1/2}{R_{a+}}\right)-\left(\frac{y-L_1/2}{R_{a-}}\right)\right],$$

$$B_z|_{line\,b} = \frac{\mu_0}{4\pi}\left(\frac{I_1(y+L_1/2)}{(y+L_1/2)^2+z^2}\right)\left[\left(\frac{x+h_1/2}{R_{b+}}\right)-\left(\frac{x-h_1/2}{R_{b-}}\right)\right],$$

$$B_z|_{line\,c} = \frac{\mu_0}{4\pi}\left(\frac{-I_1(x-h_1/2)}{(x-h_1/2)^2+z^2}\right)\left[\left(\frac{y+L_1/2}{R_{c+}}\right)-\left(\frac{y-L_1/2}{R_{c-}}\right)\right], \quad (11c)$$

$$B_z|_{line\,d} = \frac{\mu_0}{4\pi}\left(\frac{-I_1(y-L_1/2)}{(y-L_1/2)^2+z^2}\right)\left[\left(\frac{x+h_1/2}{R_{d+}}\right)-\left(\frac{x-h_1/2}{R_{d-}}\right)\right],$$

$$R_{a+} = R_{b+} = \sqrt{(x+h_1/2)^2+z^2+(y+L_1/2)^2},$$

$$R_{a-} = R_{d+} = \sqrt{(x+h_1/2)^2+z^2+(y-L_1/2)^2},$$

$$R_{c+} = R_{b-} = \sqrt{(x-h_1/2)^2+z^2+(y+L_1/2)^2},$$

$$R_{c-} = R_{d-} = \sqrt{(x-h_1/2)^2+z^2+(y-L_1/2)^2}.$$

Substituting Equation 11a into Equation 10 gives the mutual inductance

$$M_{rc} = \frac{N_1 N_2 d_L d_h}{I_1} \sum_{m=1}^{M=L_2/d_L} \sum_{n=1}^{N=h_2/d_h} \left| -B_{x_{mn}}\cos\theta + B_{z_{mn}}\sin\theta \right|. \quad (12)$$

3.2.2 Calculation and measurement

To verify the calculation method, four different cases were studied. As shown in Figure 7, the Rx coil was rotated while the Tx coil was fixed. Figure 7a shows that the Rx self-resonator was coaxially arranged with the Tx self-resonator and the center of the Rx self-resonator was $P_0(0,0,D_z)$ while the center for the other cases was $P_0(-20\,cm,0,D_z)$. Figures 7b, 7c, and 7d show that the Tx and Rx self-resonators were tilted $0°$, $90°$, and $45°$, respectively.
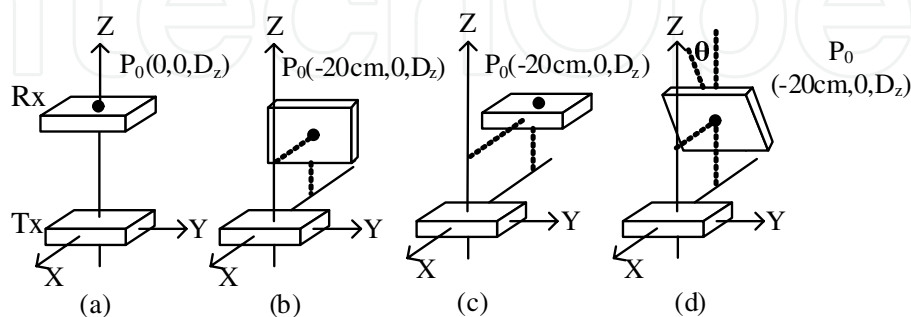

Fig. 7. Schematic drawings of four measurement setups.

In Figure 8, a Tx rectangular self-resonator fabricated in a helical type is illustrated. The Tx and Rx self-resonators were identical. The target resonant frequency was 250 kHz. 14 AWG

Fig. 8. Photograph of a rectangular self-resonator.

litz wire was used for fabrication. The size of the Tx and Rx coils was 62 cm × 33 cm × 5 cm and the number of turns $N_1 = N_2 = 19$. Some results of this study were also presented in Kim et al. (2011).

The intrinsic decay rates, capacitances of high-Q capacitors, measured self-inductances, and measured resonant frequencies of each self-resonator are shown in Table 2.

	Γ	high-Q capacitor	self-inductance	f_0
Tx	1387.5	990.9 pF	407.2 uH	249.85 kHz
Rx	1389.2	984 pF	408.5 uH	250.13 kHz

Table 2. Summary of measured parameters of each rectangular self-resonator.

Figure 9 shows the calculation and measurement results of mutual inductance according to the distance D_z between the Tx and Rx self-resonators. In calculation, the subdivisions were set to be $M = 2000$ and $N = 1000$, that is, $d_L = 0.31$ mm and $d_h = 0.33$ mm.

As shown in Figure 9, it should be pointed out that the calculation had good agreement with the measurement for each case. It is shown that with D_z smaller, the mutual inductance for the coaxial arrangement was higher than the other three cases. It can also be observed that with D_z larger, the mutual inductance for the coaxial arrangement was still the highest, while the mutual inductance for the 0° arrangement was the lowest.

4. Calculation and experimental verification

In order to verify the analysis results and design procedures of an MR-WPT system with an intermediate self-resonator, two MR-WPT systems (coaxial and perpendicular arrangements) were setup as shown in Figure 10. The Tx circular helical self-resonator was the same as that in Figure 4. The Rx self-resonator was identical with the Tx one. A spiral coil as an intermediate circular self-resonator was fabricated to reduce the volume of the MR-WPT system. The measured parameters were the same as those in Table 1. High-Q capacitors were also loaded with each self-resonator in order to adjust the target resonant frequency of each self-resonator and reduce variation of the target resonant frequency by external objects. It should be noted that the intermediate self-resonator was placed at the center between the Tx and Rx self-resonators, that is, the center of the spiral coil was $(230 \text{ mm}, 0, 0)$. Single loop coils were used as a source coil and a load coil. The transmission coefficient was measured using a vector network analyzer (Agilent 4395A). By varying the distance between the Tx self-resonator and the source coil or the Rx self-resonator and the load coil, the proper impedance matching condition for maximum power transfer efficiency was achieved. It was also found that when
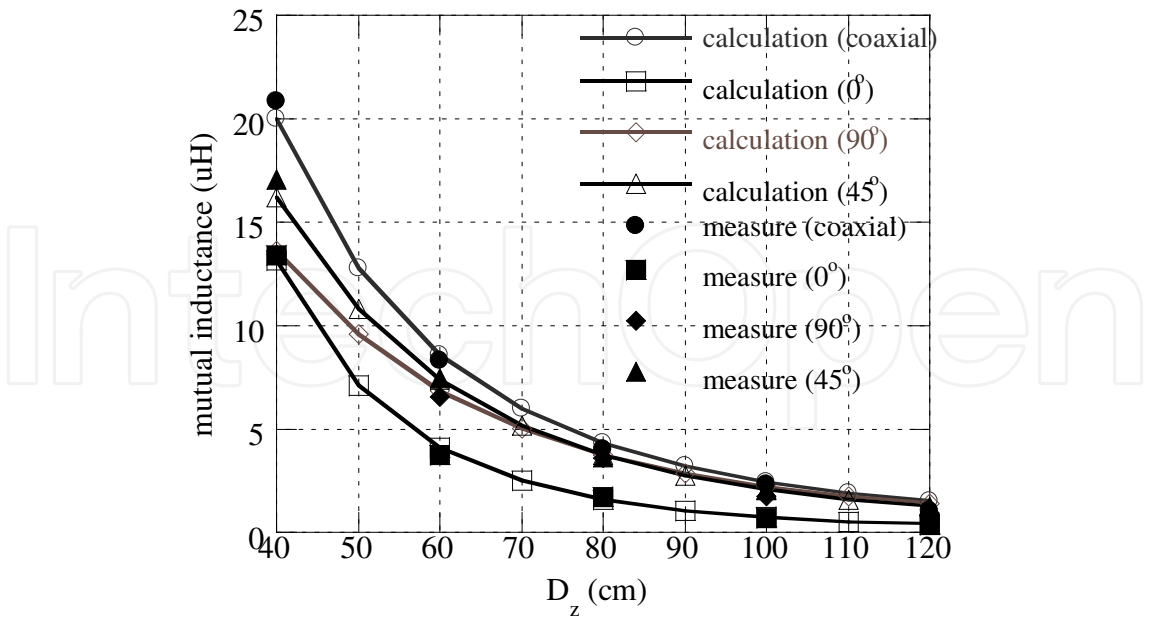
Fig. 9. Calculation and measurement of mutual inductance for both coaxial and
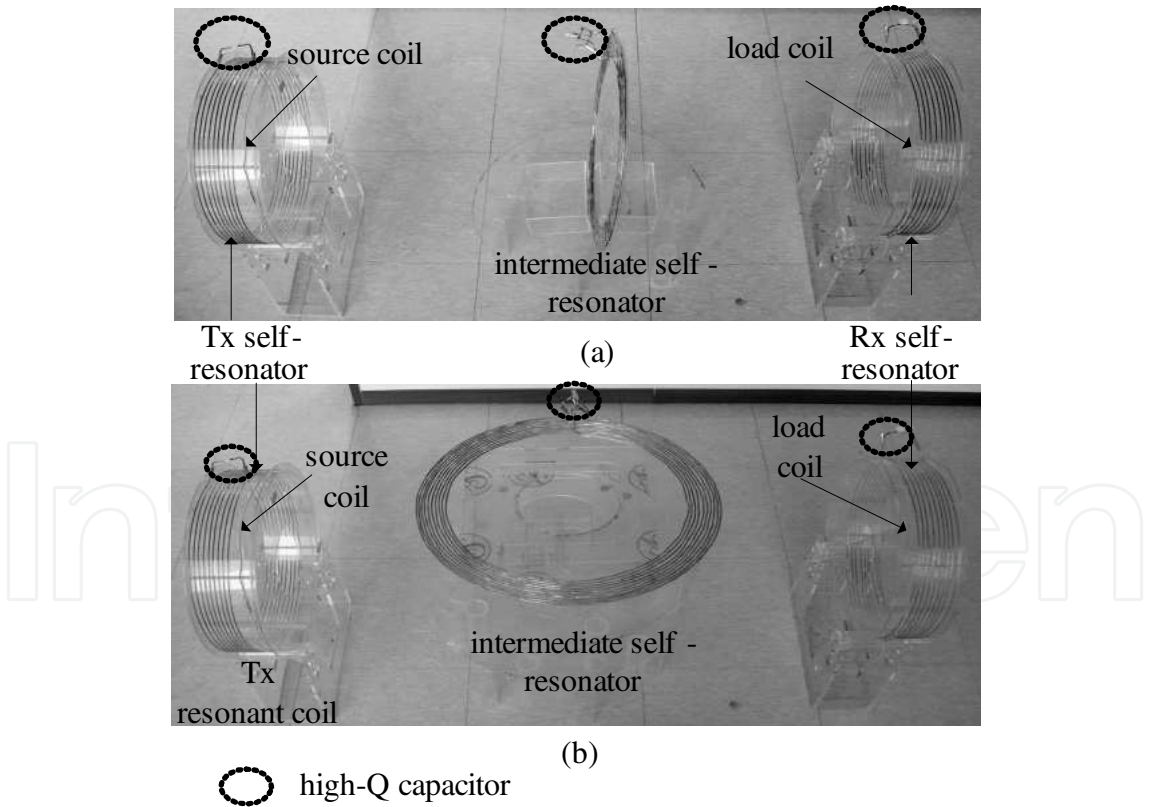perpendicular arrangements.

Fig. 10. Photograph of experimental measurement setup.

k_m was nearly five times higher than k_{12} or the distance ($2D_{1m} = D_{1m} + D_{2m}$) was more than
80 cm, k_{12} can be negligible (see Kim et al. (2011)).
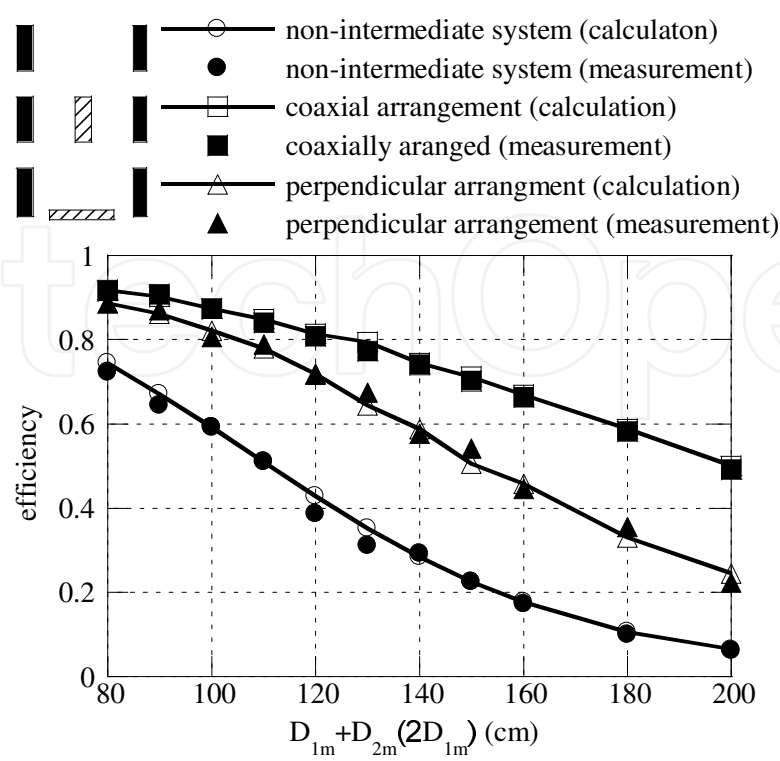In Figure 11, the measured and calculated efficiencies of two MR-WPT systems with coaxial

Fig. 11. Measured and calculated efficiencies of MR-WPT systems without an intermediate self-resonator and with coaxially arranged and perpendicularly arranged intermediate self-resonators vs. distance.
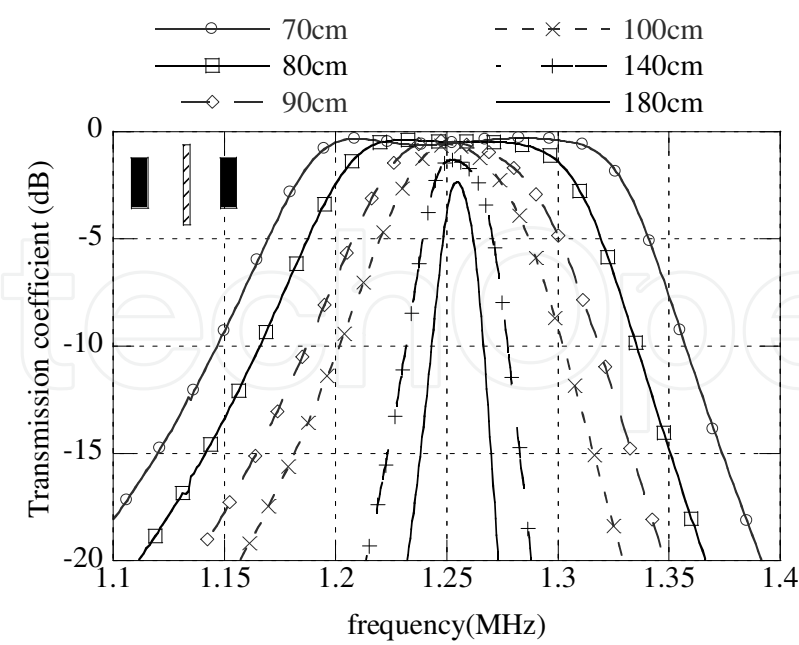

Fig. 12. Efficiency measurement of the MR-WPT system with the coaxially arranged intermediate self-resonator vs. frequency.
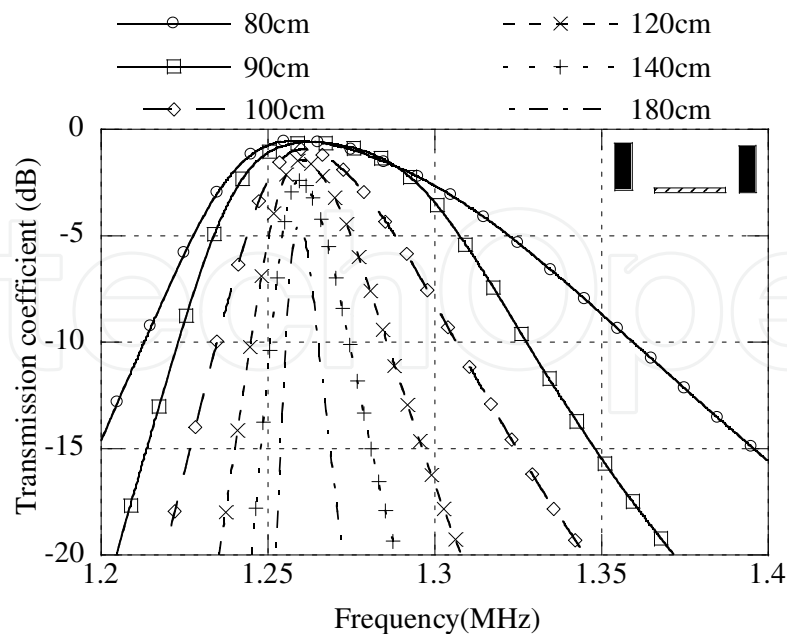
Fig. 13. Efficiency measurement of the MR-WPT system with the perpendicularly arranged intermediate self-resonator vs. frequency.

or perpendicular arrangements according to the distance between Tx and Rx self-resonators are displayed. In addition, the efficiency of an MR-WPT system without the intermediate self-resonator is displayed to make a comparison with the systems with the intermediate coil. With the aid of Equation 4, the efficiencies of the systems were calculated, and the measured parameters in Table 1 were used for calculation. As shown in Figure 11, the experimental and theoretical results were very consistent. The efficiency for the coaxial arrangement case was higher than that for the perpendicular arrangement, because the mutual inductance of the coaxial arrangement was higher as shown in Figure 5. It should be noted that the system with the intermediate self-resonator has higher efficiency than that without the intermediate self-resonator. This means that using intermediate self-resonators with low losses can help to improve power transfer efficiency and extend the coverage of wireless power transfer effectively.

Figures 12 and 13 show the measured efficiencies of the coaxial and perpendicular arrangement systems for different distances according to frequency, respectively. In the case of the coaxial arrangement, the efficiencies were nearly symmetric according to frequency while those for the case of the perpendicular arrangement were asymmetric according to frequency. The reason for this was that with a shorter distance in the perpendicular arrangement case, k_m was no higher than k_{12} and k_{12} was no longer negligible. It should also be pointed out that using intermediate self-resonators can help to make the operating frequency bandwidth broader.

5. Conclusion

In this article, the characteristics of an MR-WPT system with intermediate self-resonators were analyzed. Its power transfer efficiency was derived and the matching condition for maximum power transfer was also obtained. The calculation methods of mutual inductance between two

circular or rectangular self-resonators were presented and some calculation results were also explained. The analysis results, calculation methods, and design procedures were verified by experimental measurement. The measurements and calculations show that if intermediate self-resonators are properly used, an MR-WPT system with intermediate self-resonators transfers wireless power efficiently up to several meters. In particular, it is shown that the efficiency of an MR-WPT system with two self-resonators arranged perpendicularly is as good as that of a coaxially arranged MR-WPT system within a certain area. Therefore, it is expected that these analysis results and properties of an MR-WPT system with intermediate self-resonators can be well applied to develop various applications.

6. References

Kurs, A.; Karalis, A.; Moffatt, R.; Joannopoulos, J. D.; Fisher, P. & Soljačić, M. (2007). Wireless power transfer via strongly coupled magnetic resonances, *Science*, Vol.317, July 2007, pp. 83–86, ISSN 0036-8075.

Karalis, A.; Joannopoulos, J. D. & Soljačić, M. (2008). Efficient wireless non-radiative mid-range energy transfer, *Annals of Physics*, 323, 2008, pp. 34–48, ISSN 0003-4916.

Sample, A. P.; Meyer, A. & Smith, J. R. (2010). Analysis, experimental results, and range adaption of magnetically coupled resonators for wireless power transfer, *IEEE Transactions on Industrial Electronics*, Vol.58, No. 2, 2010, pp. 544–554, ISSN 0036-8075.

Hamam, R. E.; Karalis, A.; Joannopoulos, J. D. & Soljačić, M. (2009). Efficient weakly-radiative wireless energy transfer:an EIT-like approach, *Annals of Physics*, 324, 2009, pp. 1783–1795, ISSN 0003-4916.

Haus, H. A. (1984). *Waves and fields in optoelectronics*, Prentice Hall, pp. 197–234, ISBN 0-13-946053-5, NJ.

Good, R. H. (2001). Elliptic integrals, the forgotten functions, *European Journal of Physics*, Vol.22, 2001, pp. 119–126, ISSN 0142-0807.

Babic, S.; Sirois, F.; Akyel, C. & Girardi, C. (2010). Mutual inductnace calculation between circular filaments arbitrarily positioned in space: alternative to Grover's formula, *IEEE Transactions on Magnetics*, Vol.46, No. 9, 2010, pp. 3591–3600, ISSN 0018-9464.

Hayes, J. G.; O'Donovan, N.; Egan, M. G. & O'Donnell, T. (2003). Inductance characterization of high-leakage transformers, *IEEE Applied Power Electronics Conference and Exposition (APEC)*, pp. 1150–1156, ISBN 0-7803-7768-0, Feb. 2003, IEEE, FL, USA.

Kim, J. W.; Son, H. C.; Kim, D. H.; Kim, K. H. & Park, Y. J. (2011). Efficiency of magnetic resonance WPT with two off-axis self-resonators, *IEEE MTT-s international microwave workshop series on innovative wireless power transmission (IMWS-IWPT 2011)*, pp. 127–130, ISBN 978-1-61284-215-8, May 2011, IEEE, Kyoto, Japan.

Kim, J. W.; Son, H. C.; Kim, K. H. & Park, Y. J. (2011). Efficiency analysis of magnetic resonance wireless power transfer with intermediate resonant coil, *IEEE Antennas and Wireless Propagation Letters*, Vol.10, 2011, pp. 389–392, ISSN 1536-1225.
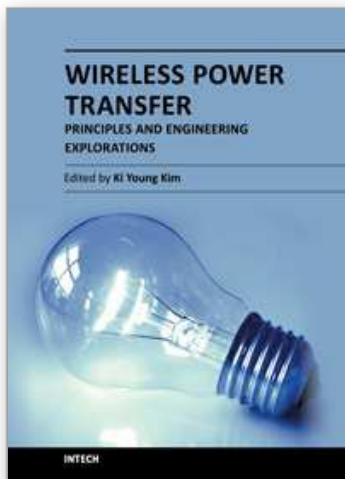
Wireless Power Transfer - Principles and Engineering Explorations
Edited by Dr. Ki Young Kim

The title of this book, Wireless Power Transfer: Principles and Engineering Explorations, encompasses theory and engineering technology, which are of interest for diverse classes of wireless power transfer. This book is a collection of contemporary research and developments in the area of wireless power transfer technology. It consists of 13 chapters that focus on interesting topics of wireless power links, and several system issues in which analytical methodologies, numerical simulation techniques, measurement techniques and methods, and applicable examples are investigated.

How to reference
In order to correctly reference this scholarly work, feel free to copy and paste the following:

Youngjin Park, Jinwook Kim and Kwan-Ho Kim (2012). Magnetically Coupled Resonance Wireless Power Transfer (MR-WPT) with Multiple Self-Resonators, Wireless Power Transfer - Principles and Engineering Explorations, Dr. Ki Young Kim (Ed.), ISBN: 978-953-307-874-8, InTech, Available from: http://www.intechopen.com/books/wireless-power-transfer-principles-and-engineering-explorations/magnetically-coupled-resonance-wireless-power-transfer-mr-wpt-with-multiplle-self-resonators

INTECH
open science | open minds